JOURNAL OF MATERIALS SCIENCE 21 (1986) 3691–3697

An electron microscope study of the amorphous magnetic material 2605 CO ($Fe_{67}Co_{18}B_{14}Si_1$)

G. A. JONES, P. BONNETT, S. F. H. PARKER
Department of Pure and Applied Physics, University of Salford, Salford M5 4WT, UK

Electrical resistivity and transmission electron microscope studies have been carried out on the primary crystallization process occurring in two batches of the amorphous alloy 2605 CO. The transformation is characterized by an activation energy of ~ 2.3 eV and a pre-exponential constant, $\ln K_0 \sim 37\ \text{min}^{-1}$. The microscope investigations show that the final dendrite size and dendrite volume density (cm^{-3}) are both temperature dependent – moreover the former is also batch dependent. On the other hand the fractional change in resistivity during the anneal seems to be a strong function of final dendrite size and is independent of batch. Observation on partially crystallized samples lends credence to the theory of a rapidly diminishing nucleation rate such that the activation energy of the whole transformation is largely determined by the activation energy associated with the growth of dendrites.

1. Introduction

Allied Corporation's metallic glass 2605 CO has useful magnetomechanical properties which make it an ideal contender for transducer devices. The fact that it often possesses a layer of surface crystallization on the wheelside of the ribbon appears not to impair these properties [1]. An electron microscope study of the surface crystallization which consists mostly of aggregates of α-iron together with β-cobalt and various borides has already been presented [2]. Transmission electron microscope investigations of thinned ribbon after various degrees of crystallization have also been reported [3, 4]. For example after annealing at 650 K Cumbrera *et al.* [3] found crystallization occurred involving the formation of Fe-rich FeCo solid solution with a lattice parameter of 0.285 nm, close to the value of 0.286 nm for α-iron. The crystallized products took the form of dendrites of a butterfly shape. At higher annealing temperatures (> 830 K) further phases may be nucleated. In this paper we shall be principally concerned with the primary transformation i.e. the first peak of a continuously heated differential scanning calorimeter trace.

Our main aim is to help correlate the crystallization kinetics as derived from resistivity data, with suitable micrographs obtained either during or at the end of the first crystallization peak. Special interest attaches to 2605 CO because, as discussed in a previous paper, [5] conventional Johnson–Mehl–Avrami (JMA) plots of $\ln \ln (1 - x_2)^{-1}$ against $\ln t$ show a non-linearity in the first peak characterized by two distinct values of the Avrami exponent ($n = 0.5$ and 2). x_2 is the transformed volume fraction and t is the annealing time. Despite this non-linearity Kissinger plots showed that the peak could be characterized by a single activation energy, Q, (typically 2.5 eV). This result was confirmed by the resistivity data used in two ways (the time to a given fraction and the change of rate methods) without recourse to any specific rate equation.

Using the electron microscope data we have made approximate estimates of dendrite size, dendrite volume density and hence total crystallization fraction as a function of time and temperature. The best accuracy is estimated at 20%. This information might give clues as to the nucleation rate and hence help elucidate the nature of the first transformation.

2. Experimental details

The set-up for the resistivity measurements has been fully described elsewhere [5]. Suffice it to say that strips some 2.5 mm in width and of length 3.4 cm were used as samples. Two different batches of 2605 CO were examined (designated hereafter as I and II), X-ray diffractometry proving that samples of II had a greater degree of initial wheelside surface crystallization than the corresponding samples of I. The upper temperature limit for the resistivity apparatus was about 400° C. Several samples of II were annealed at higher temperatures (up to 450° C) using the furnace only.

Much smaller specimens for electron microscopy were prepared by a two-stage thinning process involving initial electropolishing and then ion-thinning with 5 keV Ar^+ beams. The latter avoids the possibility of preferential electropolishing of crystalline material which invariably occurs otherwise. The electropolishing itself was done in a two jet device using 10% perchloric acid–90% acetic acid as electrolyte. The electron microscope used was a Jeol 200 CX operating at 200 kV.

3. Results

3.1. Resistivity

The results for n_1 and n_2, the initial and final slopes of the JMA plots, are given in Table I. They were presented in a previous paper [5] and are included here for reference. Generally speaking the values of n_2 increase with decreasing temperature: there is a less obvious

0022–2461/86 $03.00 + .12

TABLE I Slopes n_1 and n_2 for various anneal temperatures [5]

Sample No.	1	3	4	11	6	10
Anneal temperature (K)	661	648	638	628	623	573
Slope n_1	1.78	1.47	2.37	2.0	1.78	2.91
Slope n_2	0.21	0.38	0.48	0.58	0.53	0.82

pattern for n_1. It may be surprising to learn therefore that both sets of parameters actually give a constant value for the activation energy. Assuming that the rate constant, K, follows an Arrhenius relation

$$K = K_0 \exp(-Q/kT) \quad (1)$$

where K_0 is the pre-exponential factor, then a plot of ln K against $1/T$ will yield a slope of $-Q/k$. T is the anneal temperature and k is the Boltzmann constant. K is obtained from the y-intercepts of the JMA plots ($y = n \ln K$). Of course each JMA plot provides two values of K on account of their non-linearity. Graphs of Equation 1 are shown in Fig. 1. The slopes are virtually identical giving $Q = 2.21$ eV (from n_1) and $Q = 2.31$ eV (from n_2). These agree with each other within experimental error and also agree reasonably well with the values obtained by alternative techniques but using the same resistivity data where only a general rate equation is assumed [5, 6]. According to [1] the y-intercept of Fig. 1 gives the pre-exponential factor, ln K_0. When extrapolated to $1/T = 0$, we get ln $K_0 = 38\,\text{min}^{-1}$ (from n_1) and ln $K_0 = 36\,\text{min}^{-1}$ (fron n_2) again in good agreement. All the experimental evidence adduced therefore tends to confirm the fact that the first crystallization process does follow a JMA equation with constant values of Q and ln K_0 but two different values of Avrami exponent n.

Several authors [3, 7] have noted the fact that the change in resistivity of 2605 CO ($(\varrho_f - \varrho_i)/\varrho_i$ where ϱ_i and ϱ_f are the initial and final – i.e. when the first crystallization is completed – resistivities, respectively) is greater as T increases. Our results confirm this. The percentage change in resistivity as a function of annealing temperature is shown in Fig. 2 for several samples of I and two samples of II. This phenomenon has generally been attributed to a difference in equilibrium concentration of the matrix as the temperature is raised [3]. The implication is that the amount of iron–cobalt crystallized is a function of temperature (smaller at lower temperatures) so accounting for the differences in observed resistivity changes. Our electron micrographs indicate that this may not be the sole factor and that the morphology of the precipitated phase also plays a role.

3.2. Electron microscopy

3.2.1. Fully crystallized samples

Fig. 3 shows micrographs of samples of I annealed at 300, 350, 365 and 388° C together with a diffraction pattern of a specimen annealed at 355° C which clearly shows the b c c rings of iron. Even a cursory glance at Fig. 3 indicates that the average dendrite size decreases as the annealing temperature is raised. In general the dendrites present more of a box-like nature consisting of four quadrants rather than the butterfly morphology reported by Cumbrera *et al.* [3]. Occasionally "three legged" shapes are observed. We have attempted to estimate the average size of the dendrites at each anneal temperature – the maximum dimension of individual dendrites was measured. This is not easy, especially at higher temperatures where some impingement has occurred and the results must be treated with some reserve as there may be as much as 20% error in the measurement. Nevertheless after repeated analysis of the micrographs we have arrived at the graph presented in Fig. 4 which tends to demonstrate a linear relationship between mean dendrite dimension against temperature. It should be noted

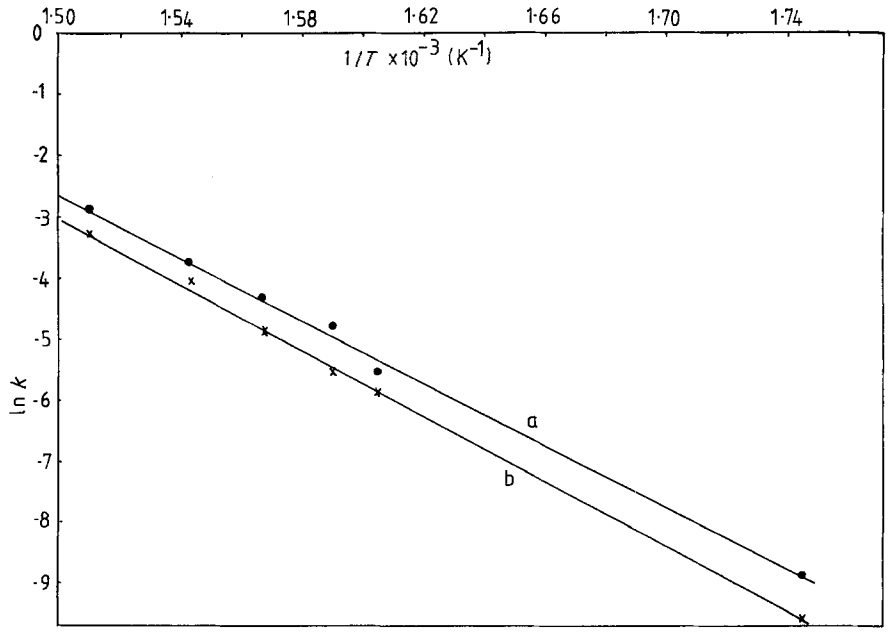

Figure 1 A plot ln K against $1/T$. Slope is Q/k and intercept at $1/T = 0$ gives in K_0; (a) obtained from n_1 values and (b) obtained from n_2 values – see Table I and the main text.

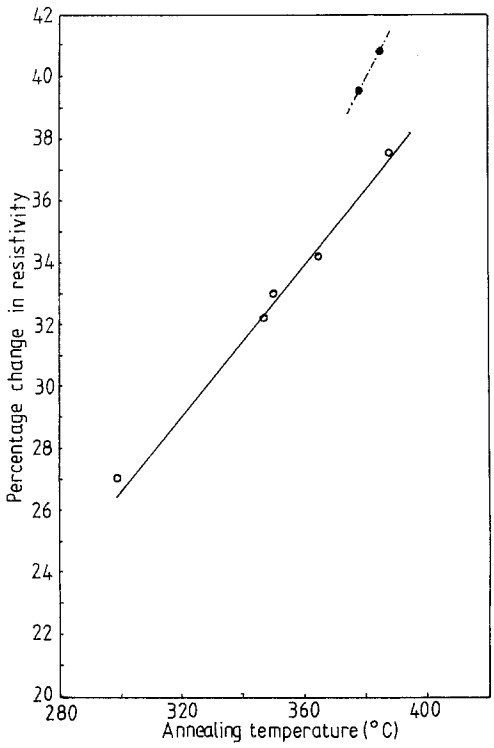

Figure 2 Percentage change in resistivity against annealing temperature in °C. (○) Samples of I; (●) samples of II.

that the average dendrite size even at 300° C is much less than the sample thickness of $\sim 30\,\mu m$.

If an analysis of dendrite dimension is difficult, then the estimation of the dendrite density, i.e. the number of particles per unit volume, N_v, presents even more problems. To begin with, the thickness of the wedge shaped foils is not known – we have assumed a reasonable value of $t = 0.15\,\mu m$ for electron transmission at 200 kV and that this is common to all the specimens. In the case of negligible overlap, N_v is given in terms of N_a, the number of particles counted per unit area of micrograph, by the relation [8]

$$N_v = N_a/(\bar{D} + t) \quad (2)$$

where $\bar{D}$ is the average dimension of the precipitates. The results of the analysis are shown in Fig. 5 where, not unexpectedly in view of Fig. 4, the volume density of dendrites increases with increasing temperature. In fact Fig. 5 reveals that some 5 to 6 times more dendrites are nucleated at 388° C compared with the number at 300° C. Once again the actual values must be considered in light of the assumptions made but we believe that the figures obtained for N_v, in the range $0.3\text{-}1.95 \times 10^{14}\,cm^{-3}$ probably represent a reasonable order of magnitude estimate.

Knowing both N_v and $\bar{D}$ a crude approximation of the fraction of the total sample crystallized may now be attempted. Noting the commonly observed square cross-section we shall simply assume that the dendrites are cubes of dimension $\bar{D}^3$. The resulting values are tabulated in Table II.

It is apparent that no trend is discernible in these results in the temperature range 350 to 388° C: in particular there is no sign that the crystallized fraction falls with decreasing temperature. This probably reflects the nature of the approximation about the volume of individual dendrites. On the other hand, the

TABLE II Fractional volume of transformed material for samples I

T(° C)	$N_v(\bar{D}^3)$
388	0.38
365	0.35
355	0.39
350	0.45
300	0.26

sample annealed at 300° C does seem to have reached a significantly lower value of $N_v\bar{D}^3$ and a scrutiny of Fig. 3d appears to bear this out. However, visual examination of micrographs can be misleading.

Turning in more detail to samples of II, they also show a temperature dependence of dendrite dimension when the first crystallization is completed. Fig. 6 shows micrographs of fully crystallized specimens at 378 and 390° C, respectively. Interestingly enough (see Fig. 4) the values of $\bar{D}$ for samples of II do not coincide with the plot for samples of I. (Incidentally, the specimen annealed at 450° C showed traces of boride). Generally speaking the dendrites in the former are smaller for a given temperature. It will be recalled that the percentage change in resistivity for II also lay on a different curve (Fig. 2). This point will be developed in the discussion section which follows. Owing to the smaller number of samples studied and the degree of overlap, no attempt was made to estimate the amount of crystallization in samples of II and to correlate it with annealing temperatures.

Finally we have calculated the standard deviation of the type I specimen dendrite dimensions in order to obtain some idea of the size distribution. Of course there is the usual problem in that the thinning method used may have sliced off pieces of dendrites on the surface and so what appear to be small dendrites may only be fragments of larger ones. However this fragmentation effect will occur for every specimen and therefore represents a constant hazard. Bearing this in mind the results, displayed in Table III, are significant. The standard deviation has been expressed as a percentage of the mean dendrite size in each case.

The Table indicates a greater spread in dendrite size at lower temperatures although on this basis the results for 365 and 350° C are juxtaposed.

3.2.2. Partially crystallized samples

Two samples of I were annealed at 358° C for 50 and 90 min in order to attain crystallization fractions, x_2, on either side of the bend in the JMA plots. Typical micrographs are shown in Fig. 7. Compared with fully crystallized samples (NB by fully crystallized is meant the completion of the first transformation), the analy-

TABLE III Size distribution of dendrites as a function of temperature

Anneal temperature (° C)	Percentage size variation
388	8.8
365	14.3
350	12.7
300	19.6

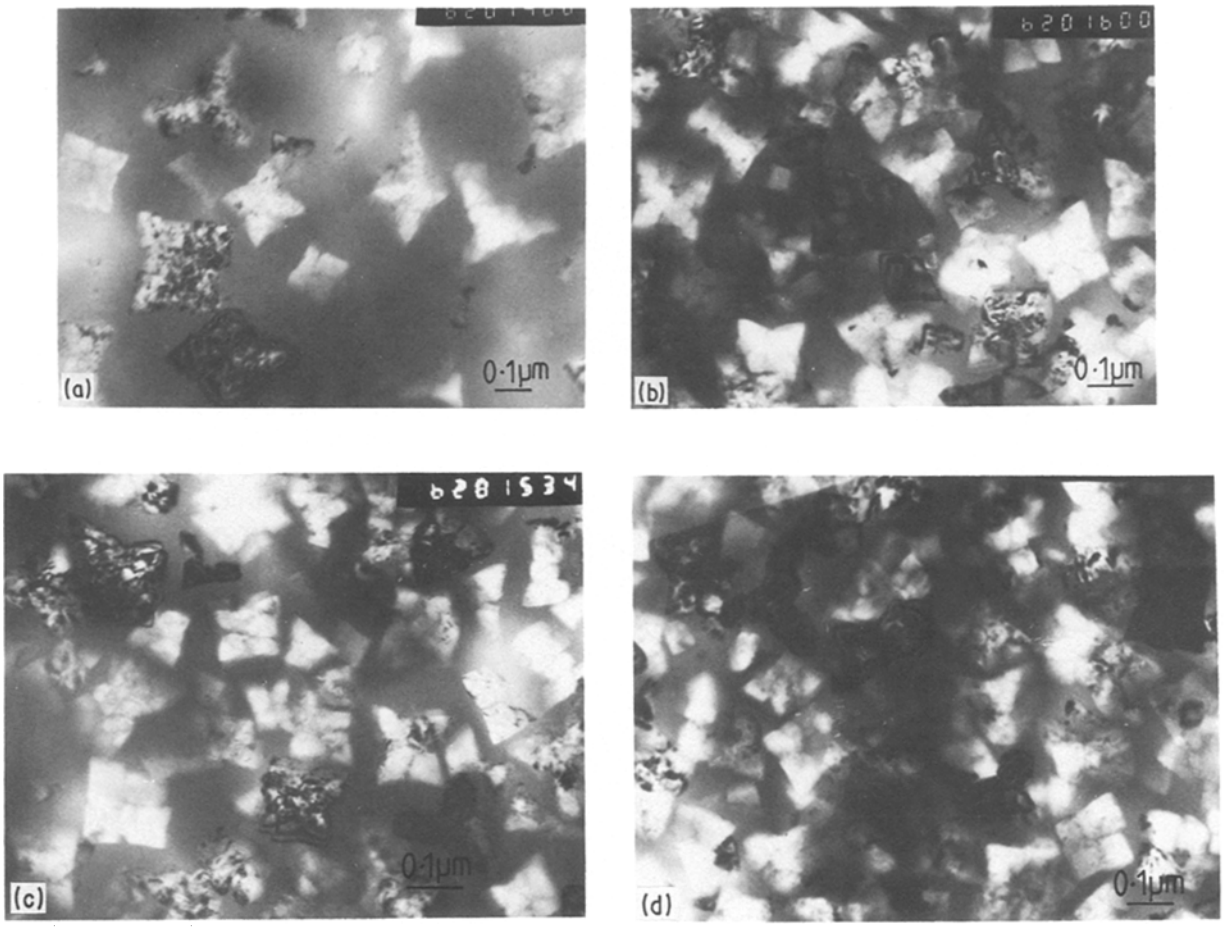

Figure 3 Specimens of I after primary crystallization at (a) 300° C; (b) 350° C; (c) 365° C; and (d) 388° C. (e) is diffraction pattern of specimen crystallized at 355° C.

sis of dendrite size and volume density is easier. This is because there is negligible overlap. As measured from the micrographs the relevant data are as follows. For the sample annealed for the shorter time $\bar{D} = 0.078\,\mu m$, $N_v = 1.267 \times 10^{14}\,cm^{-3}$ and $N_v\bar{D}^3 = 0.06$. Using the straight lines from Figs 4 and 5 the value of $N_v\bar{D}^3$ for fully crystallized samples at 358° C is 0.457. Thus the percentage of crystallization in Fig. 8a is 13%, i.e. $x_2 = 0.13$. Similarly, for the sample annealed for 90 min, $\bar{D} = 0.116\,\mu m$, $N_v = 1.274 \times 10^{14}\,cm^{-3}$, and $N_v\bar{D}^3 = 0.2$, representing a crystallized fraction of $x_2 = 0.44$. The two cases therefore do straddle the break in the JMA plot which normally occurs at about $x_2 = 0.3$.

One interesting observation about these results is that the dendrite volume density, N_v, is approximately the same for both partial anneal times: moreover as can be read off from Fig. 5, the value of N_v for samples of I fully crystallized at 358° C is $1.25 \times 10^{14}\,cm^{-3}$. In other words it appears that the volume density of dendrites remains more or less constant throughout the transformation.

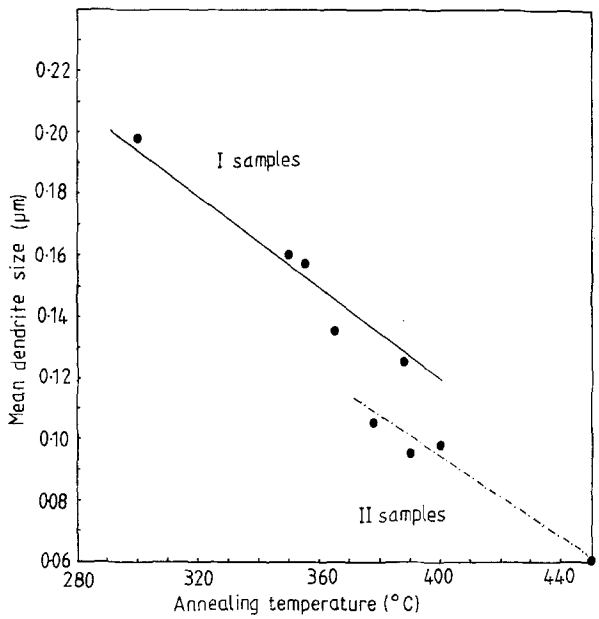

Figure 4 Mean dendrite size (μm) against annealing temperature after completion of primary crystallization for samples of I and II.

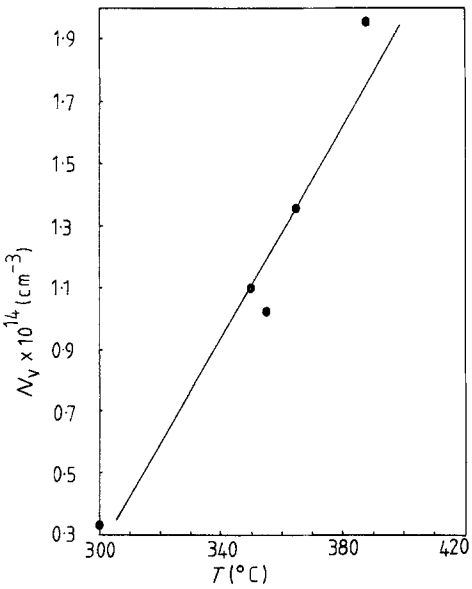

Figure 5 Dendrite volume density, N_v (in cm^{-3}) against annealing temperature T (° C) for primary crystallized samples of I.

The percentage size variation for these samples has also been evaluated and is 21.4 (x_2 = 0.13) and 24.6 (x_2 = 0.44). These are fairly close and the difference between them is probably within experimental error; nevertheless they are considerably higher than might be expected for a fully crystallized sample annealed at this order of temperature (see Table III).

Finally, by measuring the dimensions of the largest dendrite in each micrograph of Fig. 7, some idea of their growth rate can be obtained at 358° C. This turns out to be 1.8×10^{-11} m sec^{-1} which is low. For example it compares with the growth rate of $Pd_{82}Si_{18}$ at only 275° C [9].

4. Discussion and conclusions

Despite the approximation made in this paper certain conclusions are inescapable. For example there is a marked difference in dendrite dimensions and volume density – at a given temperature – between specimens of I and II. Since they were of similar thickness, the discrepancy must be attributed to the initial quenching conditions (e.g. the cooling rate) about which we have no information. It is not likely that the degree of initial surface crystallization would be significant because as was shown in [2] ribbons which had been etched of both surface layers had identical characteristics as monitored by differential scanning calorimetry.

It is also beyond dispute that the mean dendrite size attained at the termination of the primary transformation is temperature dependent – this is true of both I and II ribbons. The higher the temperature, the smaller the dendrites. This indicates that the reaction is not isokinetic, i.e. independent of thermal history. On the other hand the variation in dendrite size is compensated for by a larger value of N_v the dendrite volume density in cm^{-3}, at higher temperatures. In effect the two factors tend to balance each other with the result that, microscopically speaking it is difficult to discern any temperature variation of x_2 in type I specimens over the range 350 to 388° C. This poses a problem with regard to the observed changes in overall resistivity which as reported by other authors [3, 7] are certainly more marked the higher the temperature. Unfortunately models which predict the resistivity of composite media, e.g. that of Maxwell [10] or Landauer [11], are a function of x_2 only and independent of the size of the precipitated particles, i.e. they would predict a constant change in resistivity for a given x_2. In this respect it is useful to plot out the percentage fall in resistivity against ultimate mean dendrite size, i.e. to combine Figs 2 and 4. Fig. 8 shows the striking result that the relationship between the change in resistivity and $\bar{D}$ is linear. What is more significant is that unlike Figs 2 and 4, the data for samples I and II appear to fall on the same line which tends to suggest a fundamental relationship between the two parameters. It should be borne in mind that the change in resistivity is very accurately determined and from amongst the TEM related measurements that of $\bar{D}$ is the one least susceptible to assumptions (cf N_v and x). If these results are true it must be concluded that simple models which discount particle dimension are not capable of explaining the resistivity of a dendrite-containing matrix.

Of course, it could be argued that the estimate of x_2 from TEM micrographs is excessively crude and actually disguises a real trend of x_2 increasing with temperature. This supposition is supported by the observation that the sample annealed at 300° C has a clearly lower value of x_2. However, even if this be true Fig. 8 is hardly fortuitous and must imply that dendrite dimension plays some role in determining resistivity.

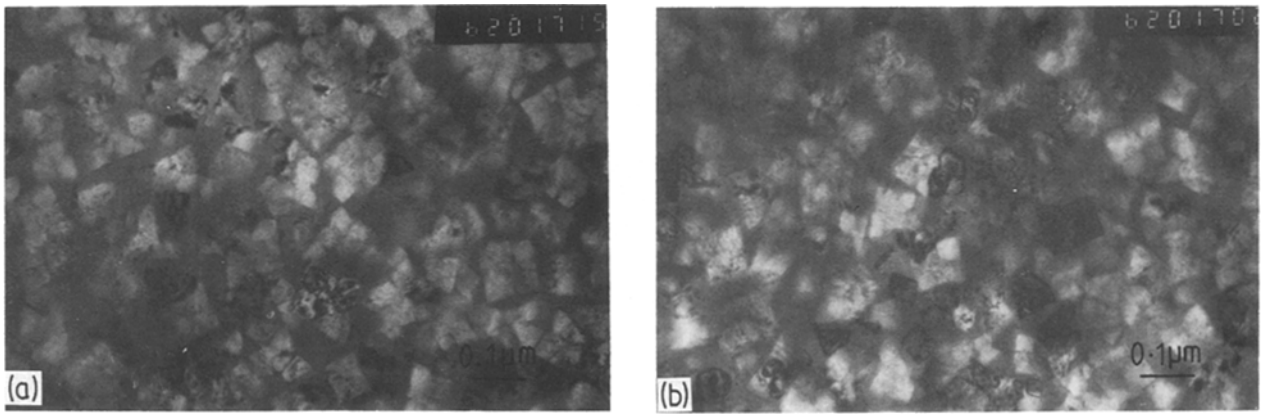

Figure 6 Specimens of II after primary crystallization at (a) 378° C; and (b) 390° C.

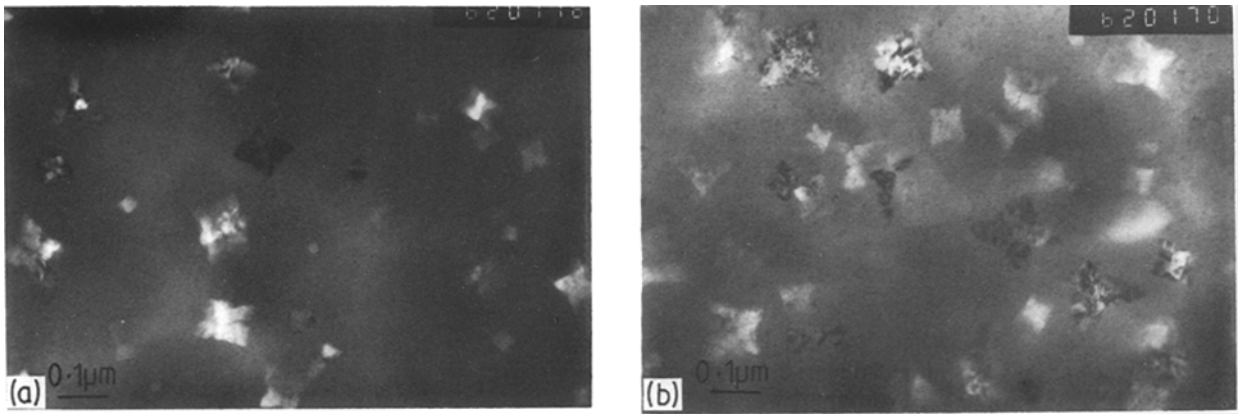

Figure 7 Partially crystallized samples of I annealed at 358° C (a) for 50 min (b) for 90 min.

Turning to the samples partially crystallized at 358° C, the results for N_v show that it differs little for $0.13 < x_2 < 1$. This probably implies nucleation at a rapidly decreasing rate such that by $x_2 = 0.13$ (50 min at 358° C) all nucleation has ceased. Such a mechanism is supported theoretically by the value of the initial Avrami exponent, n_1, which for $1.5 < n < 2.5$ indicates the diffusion controlled growth of small particles at a decreasing nucleation rate [12].

In general the activation energy for a transformation Q is a function of Q_g and Q_n the activation energies for growth rate and nucleation rate respectively. Assuming that $Q_n > Q_g$ which is usually the case in metallic glasses [13] then as the annealing temperature is raised the nucleation rate will increase faster than the growth rate resulting in a larger density of nuclei at any particular value of x_2. This temperature variation in the number of dendrites nucleated is of course observed in TEM specimens (Fig. 5).

In a diffusion controlled reaction both the nucleation rate and the growth rate fall to zero as the composition of the matrix nears its equilibrium concentration. We can express the nucleation rate as

$$v = v_0 \exp(-Q_n/kT)\, F(1 - x_2) \qquad (3)$$

If $F(1 - x_2)$ falls rapidly with x_2 so that the nucleation rate approaches zero early in the transformation then the bulk of the crystallization process would involve the growth of nuclei produced at the start of the transformation and the activation energy would be essentially constant as observed and equal to that for growth, Q_g (Fig. 1). This type of transformation should result in a small spread in the final dendrite sizes as observed experimentally.

There still remains the problem of the non-linearity of the JMA plots. Comparing the micrographs in Fig. 7 which apparently fall either side of the break, there is no obvious difference between the two at least as far as possible thickening is concerned. (The Avrami exponent is 1/2 for thickening of plates [12].) The dendrites appear to have basically the same "box type" structure at $x_2 = 0.13$ as for $x_2 = 1 -$ only the dimensions are different.

According to the formulation of the JMA equation the value of n is linked to the mechanism of the transformation and so one is looking for a distinct change in the mechanism at around $x_2 = 0.3$. Unfortunately no simple explanation for the non-linearity in terms of dendrite morphology comes readily to hand. Consequently the observed nature of the JMA plots remains unresolved at present.

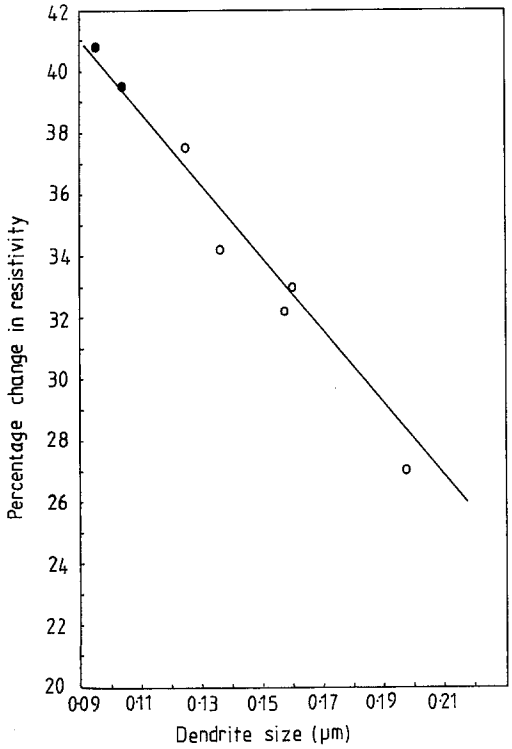

Figure 8 Percentage change in resistivity of primary crystallized samples of I and II against mean dendrite size $\bar{D}$ (in μm).

Acknowledgements

We are grateful to Allied Corporation for supplying the amorphous ribbon specimens. Also to Dr R. D. Barnard for the design of the resistivity apparatus. The work was supported by the SERC.

References

1. M. CHOI, D. M. PEASE, W. A. HINES, J. I. BUDNICK, G. H. HAYES and L. T. KABACOFF, *J. Appl. Phys.* **54** (1983) 4193.
2. G. A. JONES, S. F. H. PARKER, P. J. GRUNDY and D. G. LORD, *IEEE Trans. Magn.* **VOLMAG 20** (1984) 1381.
3. F. L. CUMBRERA, C. F. CONDE, M. MILLAN, A. CONDE and R. MARQUEZ, *J. Mater. Sci. Lett.* **2** (1983) 499.

4. E. G. BAGURAJ, G. K. DEY, M. J. PATRI and R. KRISHNAN, *Scripta Metall.* **19** (1985) 305.
5. G. A. JONES, P. BONNETT and S. F. H. PARKER, *J. Magn. Magn. Mater.* (1986), in press.
6. J. E. BURKE, in "The Kinetics of Phase Transformations in Metals" (Pergamon Press, Oxford, 1965) p. 53.
7. Y. C. KUO, L. S. ZHANG and W. K. ZHANG, *J. Appl. Phys.* **52** (1981) 1889.
8. J. A. BELK and A. L. DAVIES, (eds) in "Electron Microscopy and Micranalysis of Metals" (Elsevier, Amsterdam, 1965) p. 96.
9. K. F. KELTON and F. SPAEPEN, *Acta Metall.* **33** (1985) 455.
10. J. C. MAXWELL, in "A Treatise on Electricity and Magnetism" (Dover, New York, 1954) p. 440.
11. R. LANDAUER, *J. Appl. Phys.* **23** (1952) 779.
12. J. W. CHRISTIAN, in "The Theory of Transformations in Metals and Alloys" (Pergamon Press, Oxford, 1965) p. 489.
13. S. RANGANATHAN and M. von HEIMENDAHL, *J. Mater. Sci.* **16** (1981) 2401.

Received 6 November 1985
and accepted 10 January 1986